

DEVELOPMENT OF A HUMAN KNEE JOINT FINITE ELEMENT MODEL TO INVESTIGATE CARTILAGE STRESS DURING WALKING IN OBESE AND NORMAL WEIGHT ADULTS

Meghan K. Sylvia (1), Nicholas A. Czaplak (1), Zachary F. Lerner (3), David J. Tuttle (4), Otto J. Schueckler (5), Scott J. Hazelwood (1,2), Stephen M. Klisch (1,2)

(1) Mechanical and (2) Biomedical Engineering Departments
California Polytechnic University
San Luis Obispo, CA, USA

(3) Department of Biomedical Engineering
Colorado State University
Fort Collins, CO, USA

(4) Radiology Associates, Inc.
San Luis Obispo, CA, USA

(5) Central Coast Orthopedic Medical Group
San Luis Obispo, CA, USA

INTRODUCTION

Osteoarthritis (OA) is a degenerative condition characterized by the breakdown and loss of joint articular cartilage. While the cause of OA is not precisely known, obesity is a known risk factor [1]. Particular effort has gone towards understanding the relationship between obesity and knee OA because obesity is more strongly linked to OA at the knee than at any other lower extremity joint [2]. Although the relationship between obesity and knee OA is well established, the mechanism of pathogenesis is less understood. Excess body weight generates greater joint contact forces at the knee. However, obese individuals alter their gait, resulting in increased joint contact forces that are not proportional to body mass [3]. In this study, a partially validated knee joint finite element (FE) model was developed to predict cartilage loading during walking across individuals of varying adiposity. The model was used with kinematic and kinetic gait data to address the following hypotheses: 1) increased loading due to obesity will produce greater cartilage stress compared to the normal weight control; and 2) altered gait kinematics of obese individuals will alter the distribution of stress on the surface of the tibial cartilage.

METHODS

FE Solid Model Generation

A solid model geometry was constructed from 1.5 mm sagittal plane magnetic resonance images (MRIs) from a 33 year old healthy male with no known knee conditions. Mimics (Materialise, NV, Leuven, Belgium) was used to segment MRIs and construct 3D geometry of each bone and tissue structure. Mimics' Gaussian smoothing algorithm was used to smooth irregularities. The model included: the distal femur and proximal tibia bones; the medial collateral (MCL), lateral collateral (LCL), anterior cruciate (ACL), and posterior cruciate (PCL) ligaments; the medial and lateral menisci; and articulating cartilages of the tibiofemoral joint (Figure 1).

SolidWorks (Dassault Systemes, Velizy-Villacoublay, France) was used to assemble the model and remove any overlap between structures. FE meshes of individual structures were generated in TrueGrid Software (XYZ Scientific Applications, Inc., Livermore, California, USA) and exported to Abaqus (Dassault Systemes) for FE analysis. The femur and tibia were modeled as rigid, non-deformable shell elements due to their relatively high rigidity. All other soft tissue structures were modeled with linear 3D hexahedral elements. The ligaments were treated as transversely isotropic materials and assigned physiological material properties [4-6]. The cartilage ($E=15$ MPa, $\nu=0.475$) and menisci ($E=59$ MPa, $\nu=0.49$) were modeled as linear isotropic elastic materials [7,8].

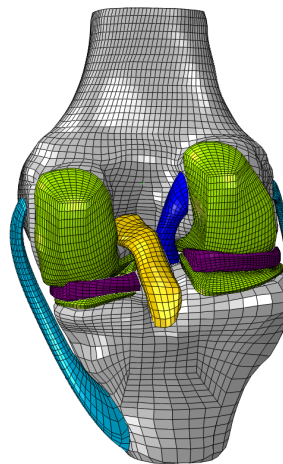


Figure 1: FE mesh of the knee.

Surface tie constraints were used to anchor cartilage and ligament structures to appropriate bony landmarks. Frictionless contact interactions were defined between the articulating surfaces of the femoral and tibial cartilages. Since the fibula is not included in this model, the distal face of the LCL was secured with linear spring elements with stiffnesses of 2.66 and 0.086 N/mm in the longitudinal and transverse directions, respectively. Spring elements were used to attach the anterior and posterior horns of the menisci to the tibial condyles. The stiffness of the meniscal springs varied from 3.2 to 5.4 N/mm [9].

Joint loads and moments were

applied to a reference node on the femur mesh approximately midway between the femoral condyles. Femur rotation in the sagittal plane was fixed at the desired flexion angle with all other degrees of freedom unconstrained. The tibia was fixed with zero degrees of freedom.

Motion Analysis and Joint Reaction Analysis

Kinematic and kinetic data was collected from normal weight (NW) and obese (OB) participants during treadmill walking at 1.25m•s⁻¹ [10]. Data from three NW and three OB individuals were averaged for this study. A weighted static optimization approach was used to predict muscle forces [10]. The resultant forces and moments were calculated using OpenSim’s Joint Reaction Analysis and represent the knee joint contact force in the FE model.

FE Model Analysis and Output

Contact pressures at 25%, 50%, and 75% of stance were analyzed to compare NW and OB cartilage stress and regions of increased loading during the gait cycle.

RESULTS

The greatest contact pressure was observed at 25% and 75% stance for OB and NW knee conditions, respectively (Figure 2). Maximum pressure reached 9.9 MPa in the OB knee at 25% stance compared to 7.4 MPa in the NW knee at 75% stance. Both OB and NW knee conditions produced the lowest contact pressure at 50% stance. At 50% stance, minimum pressure was 3.5 MPa in the OB knee and 3.1 MPa in the NW knee.

Contact pressure was greatest in the medial cartilage at all simulated phases of stance (Figure 2). The most notable difference in peak contact pressure between OB and NW knee conditions occurred at 75% stance, where medial cartilage contact pressure was greater in the NW knee than the OB knee. The OB knee condition produced more equitable contact pressure at 75% stance, with a difference of less than 1 MPa between the lateral and medial cartilage.

Contour plots show that the medial cartilage experienced the greatest contact pressure in its central region during 25% and 50% stance (Figure 3). There was increased pressure distribution along the outer edge of the medial cartilage at 75% stance. The lateral cartilage had less varied pressure distribution. Lateral cartilage contact pressure was predominately located in the central region during all simulated phases of gait. Similar trends in contact pressure distribution were observed for OB and NW knee conditions.

DISCUSSION

There were more similarities in contact pressure distribution between OB and NW knee conditions than anticipated. Experimental gait data indicated that OB individuals had smaller flexion angles, implying a more extended knee during stance. It was hypothesized that this kinematic difference would produce altered stress patterns;

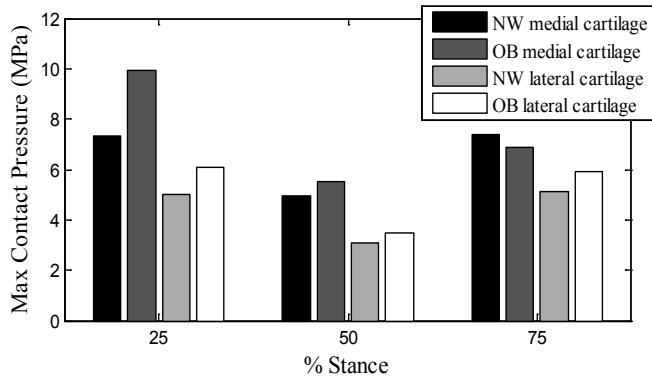


Figure 2: Maximum contact pressure on the medial and lateral tibial cartilage.

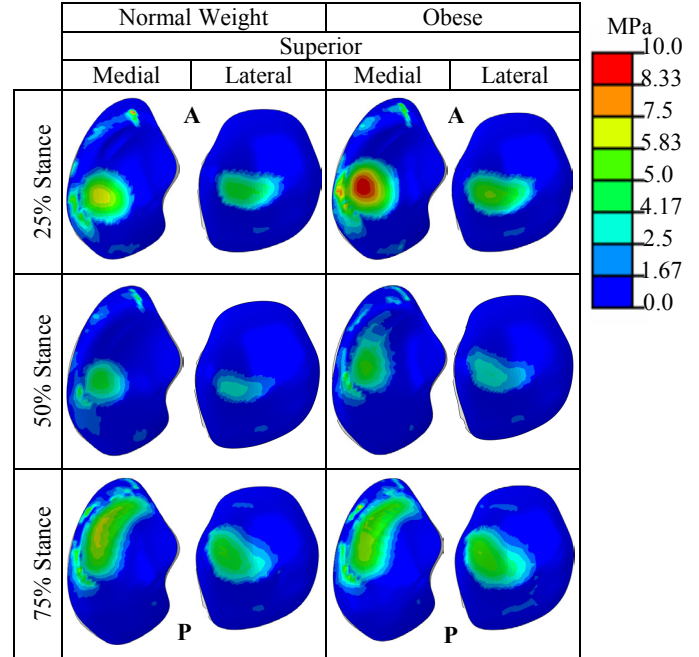


Figure 3: Contour plots of contact pressure on the lateral and medial tibial cartilage for obese and normal weight knees (A=anterior, P=posterior).

however, study results show that regions of high pressure were consistent for NW and OB knee conditions. It may be that smaller flexion angles of OB individuals result from a compensatory mechanism against larger contact forces in order to retain normal loading patterns.

Contact pressure was greater overall in the OB knee, likely due to the increase in absolute contact forces. High levels of contact stress may be associated with the development of OA; therefore, the susceptibility of obese individuals to greater than normal cartilage pressure is of concern [11]. In particular, the relative increase in contact pressure in the medial cartilage of the obese knee at 25% is indicative of a large, concentrated force acting on the cartilage surface.

The results of this study present an interesting, but limited, prediction of cartilage pressure during key points of gait; the primary limitation being that averaged data from multiple subjects was applied to a single subject specific model. Nevertheless, the results demonstrate how the use of FE modeling in combination with experimental gait data can increase the understanding of OA risk for obese patients.

ACKNOWLEDGEMENTS

Funding received from Quartus Engineering, Inc. and Cal Poly's Donald E. Bently and STRIDE Centers. The authors acknowledge Dr. Saikat Pal, for his invaluable contributions to this project.

REFERENCES

[1] Fransen, M et al., *Int J Rheum Dis*, 14:113-121, 2011. [2] Sharma, L et al., *JAMA*, 286:188-195, 2001. [3] Messier, SP et al, *Arthritis Rheum*, 52:2026-2032, 2005. [4] Weiss, J et al., *J Biomech*, 35:943-950, 2002. [5] Butler, D et al., *J Biomech*, 19:425-432, 1986. [6] Quapp, K et al., *J Biomed Eng*, 120:757-763, 1998. [7] Wangerin, S, Master’s Thesis, Cal Poly, 2013 [8] Li, LP et al., *Proc Inst Mech Eng H*, 225:888-896, 2011. [9] Karen, H et al., *J Biomech*, 43:462-468, 2010. [10] Haight, D., *J Orthopaed Res*, 32:324-330, 2014. [11] Segal, N et al., *J Orthop Res*, 27:1562-1568, 2010.